

Article

Journal of Cerebral Blood Flow & Metabolism (1997) **17**, 695–703; doi:
10.1097/00004647-199706000-00011

Measurement of Cerebral Blood Flow in Dogs with Near Infrared Spectroscopy in the Reflectance Mode Is Invalid

These studies were supported by the USPHS NIH grant NS 20020 and The Wellcome Trust, London, England (18085).

C R J C Newton^{*□}, D A Wilson^{*}, E Gunnoe^{*}, B Wagner^{*}, M Cope[□] and R J Traystman^{*}

1. Department of Anesthesiology and Critical Care Medicine, The Johns Hopkins Medical Institutions, Baltimore, Maryland, U.S.A.
2. Department of Neurosciences Unit, Institute of Child Health, University College Hospital, London, England
3. Department of Medical Physics and Biomedical Engineering, University College Hospital, London, England

Correspondence: CRJC Newton, Neuroscience Unit, Wolfson Centre, Mecklenberg Square, London, WC1N 2AP, England.

Received 15 July 1996; Revised 19 December 1996; Accepted 07 January 1997.

[Top of page](#)

Abstract

Near infrared spectroscopy (NIRS) is used to measure CBF (CBF_{NIRS}) in humans, based on Fick's principle, using oxygen as an intravascular tracer. We compared CBF_{NIRS} with CBF measured by microspheres ($CBF^{\#}$) and the venous outflow technique (CBF_v) in 15 dogs, altering CBF with ventilation-induced changes in $PaCO_2$. Five hundred forty-nine CBF_{NIRS} measurements were attempted using an integration time of 2.5 s on the saturation signal from the tongue. One hundred ninety-eight (36.1%) of the measurements fulfilled predefined criteria. The coefficient of variation (CV) for six measurements under stable conditions was 29.1%. The CBF_{NIRS} measurements correlated best with microsphere-measured blood flows in the cortical gray matter (median 0.43,

range 0.16–0.93); the contributions of the skull and dura were variable. The CBF_v varied by a median of 12% (range 0–67%) during the CBF_{NIRS} measurements. The percentage of acceptable CBF_{NIRS} measurements, the CV, and the correlation coefficients of the CBF_{NIRS} were improved by using saturation signal directly from the artery and varying the integration time with an estimate of the minimum transit time. The current method of measuring CBF_{NIRS} in the reflectance mode is inaccurate when compared with other accepted techniques.

Keywords:

Cerebral blood flow, Near infrared spectroscopy

Abbreviations:

CBF_#, CBF measured by microspheres; CBF_{NIRS}, CBF measured by NIRS; CBF_v, CBF measured by venous outflow technique; CV, coefficient of variation; DHb, deoxygenated hemoglobin; DPF, differential pathlength factor; Hb_{diff}, differential hemoglobin; HbO₂, oxygenated hemoglobin; Hb_T, total hemoglobin; mTT, minimum transit time; NIRS, near infrared spectroscopy

Near infrared spectroscopy (NIRS) measures oxyhemoglobin (HbO₂) and deoxyhemoglobin (DHb) in tissues noninvasively. NIRS has been proposed as a technique to measure CBF ([Edwards et al., 1988](#)), and since HbO₂ is used, the technique provides an indirect measure of oxygen delivery to the brain. Furthermore, NIRS can provide repeated measurements without the use of ionizing radiation.

The NIRS measurement of CBF (CBF_{NIRS}) ([Edwards et al., 1988](#)) is based upon the finding that light in the NIR region penetrates biological tissue up to 8 cm ([Jobsis, 1977](#)) and is absorbed by DHb and HbO₂. Experimentally derived algorithms have been developed that allow quantification of each of these chromophores ([Matcher et al., 1995](#)). It has been proposed that CBF can be measured by monitoring changes in HbO₂ in response to changes in inspired oxygen ([Edwards et al., 1988](#)). Previous attempts to validate this technique have demonstrated good correlation with the xenon measurement of CBF in neonates ([Skov et al., 1991](#); [Bucher et al., 1993](#)) when the optodes are placed across the head in the transmission mode; i.e., the angle subtended by the emitter and detector optodes at the center of the head is >90°. However, more recent studies have used the NIRS technique in older children ([Fallon et al., 1993](#)) and adults ([Elwell et al., 1994](#)), with the optodes placed across the forehead in the reflectance mode (angle <90°). The latter configuration is quite different from that in which the validation procedures have been performed in that light penetration into the brain will be poorer and the CBF on average will be higher. Furthermore there are two other problems with CBF_{NIRS}: over 66% of the measurements are not used as they do not fulfill preset criteria, and the coefficient of variation (CV) of the measurements is over 17% ([Fallon et al., 1993](#); [Elwell et al., 1994](#)).

We determined the validity of NIRS measurements of CBF in the reflectance mode by comparing the CBF_{NIRS} with other independent measures of CBF in dogs. We used radiolabeled microspheres to quantify steady-state CBF and regional CBF (CBF_p) and the venous outflow technique to evaluate fluctuations in CBF (CBF_v) induced by hypoxia during the NIRS measurements and examine the source of the variability in the CBF_{NIRS} .

[Top of page](#)

METHODS

NIRS theory

Changes in the concentrations of DHB and HbO₂ can be quantified using a modified Beer-Lambert law that describes optical attenuation in a highly scattering medium: [EQUATION 1](#) where OD is optical density, α the absorption coefficient of the chromophore ($mM^{-1} cm^{-1}$), c the concentration of the chromophore (mM), L the physical distance between the points where the light enters and leaves the tissue (cm), B a pathlength factor that takes into account the amount of scattering of light in the tissue, and G the factor related to the geometry and scattering coefficient of the tissue. If L , B , and G are assumed to remain constant, changes in concentration of the chromophore will be proportional to the changes in optical density. The absorption coefficients of HbO₂ and DHB have been derived ([Cope, 1991](#); [Matcher et al., 1995](#)) and corrected for wavelength-dependent pathlengths ([Essenpreis et al., 1993](#)). The pathlength factor has been measured in the heads of rats and humans ([van der Zee et al., 1992](#)) and is relatively constant when the interoptode distance is >2.5 cm in the reflectance mode ([van der Zee et al., 1992](#); [Ferrari et al., 1993](#)).

$$\text{Attenuation (OD)} = \alpha \cdot c \cdot L \cdot B + G$$

CBF_{NIRS}

The CBF_{NIRS} is based on Fick's principle using oxygen (O₂) as the intravascular tracer ([Edwards et al., 1988](#)). According to Fick's principle, the rate of accumulation (Q) of a tracer substance in an organ is equal to the difference between the rate of arrival and rate of departure of that substance: [EQUATION 2](#) where $Q(t)$ is the amount of the tracer in tissue, F is flow, and C_a and C_v are the concentrations of the tracer in arterial and venous blood, respectively. If the measurements of the rate of accumulation of the tracer are made within the minimum transit time (mTT) of the tracer through the brain, then the venous outflow concentration will be zero. Thus CBF can be calculated from the ratio of the quantity of tracer accumulated to the quantity of tracer introduced during time t : [EQUATION 3](#) With a sudden increase in arterial oxygen saturation ($\Delta S_a O_2$), the initial increase in cerebral HbO₂ concentration represents the accumulation of the tracer Q . The quantity of tracer introduced is the product of the integral of $\Delta S_a O_2$ with respect to time and the arterial Hb concentration. Thus CBF can be calculated in milliliters per 100 g per minute from the following equation: [EQUATION 4](#) where K is a constant reflecting the

molecular weight of Hb, cerebral tissue density, and concentration of Hb in the subject's blood. The signal/noise ratio of the NIRS data can be improved by measuring the change in the difference between HbO₂ and DHb, i.e., [Hb_{diff}] = [HbO₂] - [DHb], since if the total Hb concentration ([Hb_T] = [HbO₂] + [DHb]) is constant, then the changes in HbO₂ and DHb will be equal and opposite and the difference between these changes will be twice the amplitude of the changes of HbO₂. Thus the equation becomes [EQUATION 5](#)

$$Q(t) = F^* \int_0^t (C_a - C_v) dt$$

$$F = \frac{Q(t)}{\int_0^t P_a(t) dt}$$

$$\text{CBF (ml 100 g}^{-1} \text{ min}^{-1}) = \frac{\Delta(\text{HbO}_2)}{K \int_0^t \Delta S_a \text{O}_2 dt}$$

$$\text{CBF (ml 100 g}^{-1} \text{ min}^{-1}) = \frac{\Delta(\text{Hb}_{\text{diff}})}{2 K \int_0^t \Delta S_a \text{O}_2 dt}$$

General procedure

Sixteen mongrel male dogs (20–30 kg) were anesthetized with sodium pentobarbital (35 mg kg⁻¹ i.v.) and mechanically ventilated, using one cylinder of a dual cylinder ventilator (Harvard model 618). The dogs were paralyzed with pancuronium (0.1 mg kg⁻¹) and anesthesia was maintained with sodium pentobarbital.

Surgical preparation.

Catheters were placed via a femoral artery into the left cardiac ventricle for microsphere injection, in the other femoral artery for withdrawal, a brachial artery for monitoring MABP, and a femoral vein for administration of drugs and fluids. In 10 of 16 dogs, an omocervical artery was cannulated for an arteriovenous fistula created to continually pass whole blood through a specially constructed oximeter and return it to the other femoral vein. In 8 of 16 dogs the confluence of the sagittal sinus, the straight vein, and lateral cerebral sinuses were cannulated for the measurement of CBF_v ([Rapela and Green, 1964](#)). In all animals, the scalp and temporalis muscle overlying the cranial vault were surgically reflected. The optical probes were placed 3–5 cm apart on the skull, ensuring that they were positioned posterior to the frontal sinuses and up to 1 cm anterior to the bregma on the left side. The optodes were shielded from ambient light with NIR opaque modeling clay and a black plastic bag placed over the whole head.

Instrumentation.

The NIRO 500 (Hamamatsu Photonics, Hamamatsu, Japan) was used in these studies. It uses pulsed laser diodes at four wavelengths (779, 828, 839, 913 nm) as its light source and a photomultiplier tube for detection. The changes in HbO_2 and DHb were calculated using an established four-wavelength algorithm ([Matcher et al., 1995](#)). The data were collected every 0.5 s during CBF_{NIRS} measurements.

Peripheral SaO_2 was monitored with a pulse oximeter (Nellcor, U.S.A.), modified to measure in the beat-to-beat mode, and the sensor was applied to the tongue. The central SaO_2 was monitored with an oximeter constructed in this laboratory that measured changes in light at 660 nm (transmitted through an in-line catheter placed between the omocervical artery and femoral vein). Regular measurements of arterial SaO_2 were made throughout the experiment and the results were used to calibrate both oximeters. The data from the oximeters were not used if there was not a substantial linear relationship (regression analysis, $r^2 < 0.80$) between the oximeters and the co-oximeter measurements.

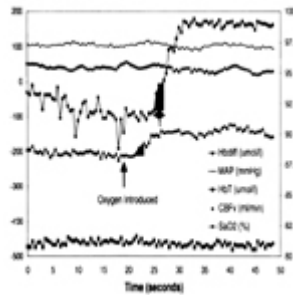
CBF measurements

CBF_{NIRS} measurements.

CBF_{NIRS} was measured by inducing mild hypoxia (S_aO_2 85–96%) with the inspiration of 13% O_2 /87% N_2 . When a steady SaO_2 baseline had been achieved, a bolus of O_2 was delivered by switching from the cylinder delivering the hypoxic mixture to the cylinder with 100% O_2 flowing through it. The switch was made near the endotracheal tube so that the change was as close to a step change as possible. CBF_{NIRS} was calculated from [EQUATION 5](#) by measuring the area under the rise in SaO_2 over the integration time

(shaded portion in [Fig. 1](#)) and regressing the result against the change in Hb_{diff} . The CBF_{NIRS} measurements were considered acceptable if they fulfilled the following criteria based upon previous studies ([Edwards et al., 1988](#); [Elwell et al., 1994](#)): (a) The SaO_2 baseline before the introduction of oxygen was between 85 and 96% saturation and varied only by one point $>2\%$ during the 5 s immediately prior to the takeoff point ([Fig. 1](#)); (b) the SaO_2 rose by at least 1%/s; (c) the change in the ratio of the Hb_T/Hb_{diff} was <0.25 during the measurement; (d) the change in end-tidal CO_2 was $<5\%$ during the measurement; (e) the change in MABP was <5 mm Hg during the measurement.

Figure 1.



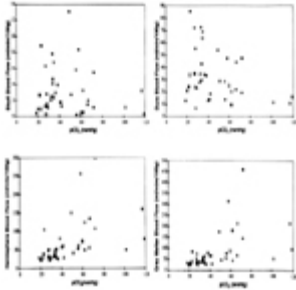
Measurement of CBF with NIRS. Panel shows changes in parameters during CBF measurement: peripheral SaO_2 signal, with calculation of the amount of tracer introduced (shaded area) in time t ; Hb_{diff} ($HbO_2 - DHb$), Hb_T ($HbO_2 + DHb$), MABP, and CBF_v . Arrow shows time when oxygen was introduced. See text for abbreviations.

[Full figure and legend \(170K\)](#)

At least six NIRS measurements were made for each microsphere measurement and $PaCO_2$ level. The means of the accepted values were used for comparison with the microsphere measurements. The single accepted measurements were compared directly with the CBF_v . A differential pathlength factor (DPF) of 4.39 was used for the calculations, based upon neonates and other animals ([Cope, 1991](#)).

In eight dogs CBF_{NIRS} was calculated in four different ways: (a) with the peripheral signal and a standard integration time (t) of 2.5 s; (b) with the peripheral signal and t altered according to an estimate of the mTT based upon previous indocyanine green measurements ([Fig. 2](#)); (c) with the central signal and $t = 2.5$ s; (d) with the central signal and $t =$ estimated mTT.

Figure 2.



PaCO₂ versus regional blood flow, measured by microspheres. Each symbol represents a single experiment. Blood flow through the outermost cortical core sample and the hemisphere was sensitive to changes in arterial PaCO₂. In contrast there was no relationship between blood flow and PaCO₂ in the skull and dura.

[Full figure and legend \(136K\)](#)

CBF_μ measurements.

Regional CBF values were measured with radiolabeled microspheres using the reference sample method ([Heymann et al., 1977](#)). Microspheres were injected into the left cardiac ventricle, and the reference blood sample withdrawn from a brachiocephalic artery using a Harvard withdrawal syringe pump. Intraventricular pressure recordings were taken before and after each injection to verify that the left ventricular catheter was in position at the time of the injection. Approximately 4×10^6 microspheres of six isotopes, ¹⁵³Gd, ¹¹⁴In, ¹¹³Sn, ¹⁰³Ru, ⁹⁵Nb, and ⁴⁵Sc, were injected in random sequence in each animal ([Marcus et al. 1976](#)).

At the conclusion of the experiment, the animal was killed by intravenous potassium chloride injection. The brain was removed and placed in 10% buffered formalin for 2–7 days. Samples of bone (>2 g) and the dura over the left hemisphere were also taken. The left and right halves of the brain were dissected into discrete areas: gray matter (cortical gray matter and caudate nucleus), white matter, and a core of brain tissue cut from the brain situated between the NIRS probes. This core was horizontally sectioned into five slices (designated core 1–5) ≈ 1 mm thick. The outmost slice (core 1) consisted of cortical gray matter, while gray matter flow consisted of blood flow measured in both cortical and deep gray matter (e.g., basal ganglia). Slices 2–5 consisted of blood flow of varying combinations of white and gray matter measured at different depths, since the depth of penetration of NIR light into the brain is an unknown variable. After weighing, the tissue samples were placed in counting vials and counted in a United Technologies Packard autogamma series 5000 scintillation spectrometer with appropriately positioned energy window settings for the isotopes. Window counts were corrected by application of an algorithm that utilizes experimentally determined overlap coefficients to correct for overlapping areas of the energy spectrum among isotopes. CBF values were calculated

from the following equation: [EQUATION 6](#) where CBF is regional CBF ($\text{ml } 100 \text{ g}^{-1} \text{ min}^{-1}$), C_B is brain tissue counts, RBF is reference blood sample withdrawal rate (ml min^{-1}), C_R is counts in the reference arterial blood sample, and W is tissue weight (g).

$$\text{CBF} = \frac{100(C_B \times \text{RBF})}{C_R \times W}$$

CBF_v measurements.

The CBF_v was used to monitor CBF during the hypoxic swings required for the NIRS measurements and to determine the predictive interval of the CBF_{NIRS} since this technique has less intrinsic variability than the microsphere technique. Briefly, the confluence of the cerebral sinuses was cannulated, the lateral sinuses were occluded with bone wax, and the blood drained was diverted through a calibrated electromagnetic flow probe (Biotronix) before being returned to the dog via the femoral vein ([Traystman and Rapela, 1975](#)). The readings from the probe were calibrated before and after the set of six NIRS measurements.

Experimental protocol

The CBF level was changed by either altering ventilation or adding carbon dioxide (CO₂) to the inspired air mixture. Measurements of CBF_{NIRS} and CBF_μ were attempted only if the end-tidal CO₂ was stable for at least 15 min, switching from one side of the ventilator cylinder delivering the hypoxic mixture to the ventilator cylinder containing 100% oxygen caused no changes in end-tidal CO₂, MABP was stable, and in the dogs prepared for the CBF_v technique, the CBF_v was stable. Fifteen to thirty minutes before measuring CBF, the animal was given pancuronium (0.1 mg/kg), pentobarbital, fluid, and sodium bicarbonate [$\text{ml NaHCO}_3 = (\text{base excess} \times 0.3)/2$], if deemed necessary. Arterial blood samples were withdrawn from the brachial artery catheter at the nadir of SaO₂ and after the 100% O₂ was administered during the first and last CBF_{NIRS} measurements and before each microsphere measurement at each PaCO₂ level. The blood was used to determine pH, PaO₂, and PaCO₂ (ABC-3 Radiometer, Denmark), O₂ content, hemoglobin content, hemoglobin saturation (OSM3 Hemoximeter, Radiometer, Denmark), glucose, and lactate (2300 Stat Yellow Springs). The measurements on the Hemoximeter were performed with the machine calibrated for dog blood.

Three CBF_{NIRS} measurements were made, then a microsphere measurement was made at the nadir of SaO₂ of the fourth CBF_{NIRS} measurement, followed by at least two additional CBF_{NIRS} measurements. The CBF_{NIRS} measurements were considered only if the animal remained stable without fluctuations in end-tidal CO₂ and MABP during the 30–45 min required to perform six CBF_{NIRS} measurements and a microsphere measurement. The

validities of the CBF_{μ} and CBF_v were assessed by comparing these with each other. To determine the CV of the CBF_{μ} , three sets of microspheres were injected within 2 min in animals that were hemodynamically stable. The CBF_v measurements were correlated with the CBF_{μ} for comparison with the CBF_{NIRS} measurements.

Data analysis

Each of the CBF_{NIRS} measurements was inspected to determine if it fulfilled the criteria stated previously. The mean and standard deviation of the CBF_{NIRS} measurements were calculated for each microsphere measurement at each P_aCO_2 level. The CV was calculated from the standard deviation/mean and expressed as a percentage. Results were analyzed on an experiment-by-experiment basis by visual inspection and by correlation analysis, since the underlying hypothesis to be tested was that the CBF_{NIRS} and either CBF_{μ} or CBF_v should be proportionally related with all data pairs falling on a straight line, preferably the line of identity in each animal. We used the correlation coefficient to compare the strength of the relationship between the NIRS measurements and the regional blood flow in the different animals and compare the CBF measured by the different techniques. Linear regression analysis was performed for the calibration of the oximeters. The Student *t* test was used to compare microsphere-measured blood flow between the two sides.

[Top of page](#)

RESULTS

CBF_{μ} measurements

Whole-brain blood flow ranged from 14 to 290 ml 100 g⁻¹ min¹. The median CV of the whole-brain blood flow in four animals in which three microsphere measurements were made under stable conditions was 11.16% (range 1.16–13.65%). There was no difference in the CV of the blood flow between the regions, including the dura and bone. In seven preparations in which the CBF was measured by microspheres and the venous outflow, the median correlation coefficient between these two techniques was 0.94 (range 0.77–0.98).

In the eight preparations with CBF_{μ} and CBF_{NIRS} measurements that maintained responsiveness to $PaCO_2$ throughout the experiment, the blood flow in left gray matter and left core 1 tissues responded more than any of the other tissues to changes in $PaCO_2$, while the blood flow in skull and dura showed little consistent response to $PaCO_2$ ([Fig. 2](#)). There were no significant differences in the CBF_{μ} measured in the gray matter, hemisphere, or core tissue samples between the sides (Student's *t* test, $p > 0.05$).

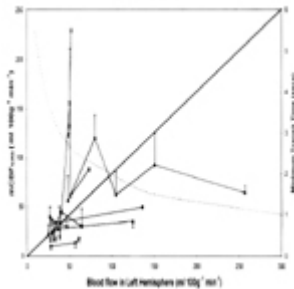
CBF_{NIRS} measurements

The optodes were placed 4.02 ± 0.48 cm apart on the left skull.

Five hundred forty-nine CBF_{NIRS} measurements were attempted in 16 dogs using the peripheral hemoglobin saturation signal with an integration time of 2.5 s. Only 198 (36.1%) measurements were considered to be acceptable using our selection criteria. The remaining 351 measurements were rejected because (a) SaO_2 baseline was unstable (23.3%), (b) SaO_2 baseline was $<85\%$ (8.0%), (c) SaO_2 rose poorly (19.3%), and (d) Hb_T/Hb_{diff} ratio changed by >0.25 (23.0%). The CBF_{NIRS} ranged from 9.89 to 229.2 ml $100\text{ g}^{-1}\text{ min}^{-1}$ and the CV of the measurements had a median of 29.1% (range 3.8–102.9%).

In the eight dogs in which CBF_{NIRS} could be calculated from the peripheral signal at three or more different microsphere measurements, the peripheral signal correlated best with the microsphere flows in first slice of core tissue (left core 1), i.e., cortical gray matter (median 0.43, range 0.16–0.93) and left hemisphere (median 0.34, range 0.18–0.88) ([Table 1](#)). Although the median correlation coefficient between the CBF_{NIRS} and microsphere flow in the data was 0.79, the range included negative correlation in three animals. The order of the tissue correlation coefficients in the tissues varied between the animals. In the comparison with the CBF_{μ} in the left hemisphere, the CBF_{NIRS} measurements fell away from the line of identity ([Fig. 3](#)), particularly at higher flows ([Fig. 4](#)).

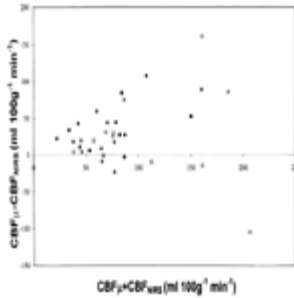
[Figure 3.](#)



Blood flow in the left hemisphere measured by microspheres plotted against mean CBF_{NIRS} ($mCBF_{NIRS}$) and estimated minimum transit time (dotted line) derived from previous experiments. Each symbol represents a single experiment. Error bars representing 1 SD are shown for the $mCBF_{NIRS}$ when there were three or more acceptable runs.

[Full figure and legend \(106K\)](#)

[Figure 4.](#)



Difference between the blood flow in left hemisphere measured with microspheres (CBF_{μ}) and mean CBF_{NIRS} ($mCBF_{NIRS}$) plotted against the average of CBF_{μ} and $mCBF_{NIRS}$, showing an increase in the difference as CBF increases. Each symbol represents a single experiment.

[Full figure and legend \(83K\)](#)

[Table 1 - Correlation coefficients of blood flow.](#)

[Full table \(\)](#)

The correlation coefficient, CV, and number of acceptable CBF_{NIRS} measurements were improved by using the central saturation signal instead of the peripheral saturation signal and altering the integration time to take into account the change in transit time estimated from microsphere measurements ([Table 2](#)). The CBF_{NIRS} correlated best with the left core 1 and left gray matter regardless of the method used to calculate the CBF_{NIRS} .

[Table 2 - Comparison of the different methods of measuring mean \$CBF_{NIRS}\$ with CBF measured by microspheres \(\$CBF_{\mu}\$ \) and single \$CBF_{NIRS}\$ and venous outflow \(\$CBF_v\$ \).](#)

[Full table \(\)](#)

CBF_{NIRS} and CBF_v

The correlation between the individual CBF_{NIRS} and CBF_v was worse than that between the mean CBF_{NIRS} and CBF_{μ} . The percentage change in the CBF_v during the entire CBF_{NIRS} measurement (i.e., the induction of hypoxia and the administration of 100% O_2) did not correlate with the minimum arterial content or the minimum SaO_2 during the measurement, although changes occurred only when the SaO_2 was $<96\%$. The percentage change also did not correlate with the amount of change in arterial content or SaO_2 during the measurement or the change in Hb_T during the Hb_{diff} increase.

[Top of page](#)

DISCUSSION

NIRS is a potentially exciting technique for measuring CBF, since it may directly measure oxygen delivery to the brain. We found that NIRS detects blood flow in the brain, but this method using oxygen as an intravascular marker in the reflectance mode is an inaccurate measure of CBF. The correlations between the CBF measured by NIRS using the SaO_2 signal from the peripheral tissues and a fixed integration time (used in clinical studies), and the CBF measured by microspheres ([Fig. 3](#)) or cerebral venous outflow technique are poor. The correlation was improved by using the central SaO_2 signal directly from an artery and varying the integration time with an estimate of the mTT. Even with these improvements, CBF_{NIRS} tended to underestimate the CBF.

The CBF_{NIRS} method using oxygen as an intravascular marker correlated with xenon measurements of CBF in neonates ([Skov et al., 1991](#); [Bucher et al., 1993](#)). Neonates have low CBF ($10\text{--}30\text{ ml } 100\text{ g}^{-1}\text{ min}^{-1}$), which is associated with long transit times ([Fig. 3](#)), so that the accuracy of the measurements can be improved by examining more data points and allowing a larger input of tracer within the mTT. Furthermore it is possible to position the optodes in the transmission mode in neonates, thereby reducing the extracranial contamination to that of the xenon method. We examined the CBF_{NIRS} method in the reflectance mode since this is required for older children and adults.

The discrepancies between the CBF_{NIRS} and the other methods for measuring CBF could be caused by changes in the DPF, extracranial contamination, changes in CBF, or consumption of the intravascular marker, oxygen, during the measurements. The DPF is essential for the quantitative measurements of the chromophores. It takes into consideration that the distance light travels is further than the spacing between the optodes, since the light is scattered by the tissue. The DPF depends upon the optical properties of the tissue and the measurement geometry. The contribution of the skull to the DPF in transmission across a rat's head as measured by time of flight was near 10% ([Delpy et al., 1989](#)). However, in the reflection mode across the larger head of the dog, the contribution of the skull to the DPF may be greater ([Hiraoka et al., 1993](#)). We were not able to measure the DPF, but used an estimate of 4.39 based upon other experimental data ([Cope, 1991](#)). This may account for the underreading of the CBF_{NIRS} compared with the CBF_{μ} in [Fig. 3](#), but would not affect the correlation coefficients or account for the nonlinear variation with blood flow. The DPF varies considerably between subjects; in rats the mean and standard deviation were 5.26 and 0.31, respectively ([Delpy et al.,](#)

1989). The DPF also varies with changes in the amount of DHb and HbO₂, although in the rat and the human the changes induced by breathing 12–100% oxygen were <6% (Delpy et al., 1989; Ferrari et al., 1990). Thus, although we could not measure the DPF, changes in the DPF should have little effect on the interpretation of results within an animal.

An important consideration of the NIRS measurements of cerebral hemodynamics in the reflection mode is the amount of extracranial contamination. By altering the CO₂, we were able to change the blood flow in the intracranial compartment without significant changes in the extracranial compartment (Fig. 2). These data suggest that the extracranial compartments (skull and dura in these preparations) make a variable contribution to the CBF_{NIRS} in the animals, since in some animals the microsphere-measured flows in the skull and dura correlated best with the NIRS measurements, while in other animals the correlation was the least compared with other tissues. Thus the median correlation coefficient of the measurements between the NIRS and dural blood flow was 0.79, but the range (-0.73 to 0.94) included three negative correlation coefficients. Overall, however, the most reliable correlations occurred between the CBF_{NIRS} and the microsphere flows in core 1, i.e., cortical gray matter, hemisphere, and whole brain (Table 1), suggesting that NIRS detects intracranial blood flow. The order of the correlations, however, among these tissues varied between animals, suggesting that the contribution of the different tissues to the NIRS signal varied with animal. This, together with the differences in the DPF, makes comparisons between subjects difficult.

The CVs of the NIRS measurements are high, both in clinical studies (Skov et al., 1991; Bucher et al., 1993; Elwell et al., 1994) and in this study. This could be caused by (a) the quality of the peripheral signal, from which the amount of tracer introduced into the system is calculated; (b) the measurements not taking place within the mTT; (c) changes in CBF secondary to the hypoxia induced for the measurement; (d) loss of oxygen within the mTT; and (e) changes in the distribution of the NIR signal with CBF.

Most clinical studies have used a saturation monitor attached to an ear or finger to detect the changes in SaO₂. The quality of the SaO₂ signal is important since 43% of the CBF_{NIRS} measurements had to be excluded because the SaO₂ baseline was not stable or the rise in the SaO₂ was not smooth. We found that the percentage of rejected measurements was reduced by using the signal direct from an artery.

One of the prerequisites of this method is that the calculations must occur within the mTT, so that the venous outflux is zero. By altering the calculations to include an estimate of the mTT, the correlation between the NIRS measurements and the microspheres or CBF_v was improved and the number of unsuccessful measurements and CV was reduced. Although the mTT can be measured with the NIRS using indocyanine green (Ferrari et al., 1992), the bolus has to be delivered into the carotid circulation, as a large bolus into the venous circulation does not provide a good-quality signal in the head.

The Fick principle assumes that there is no consumption of the tracer within the measurement period. There is evidence that oxygen diffuses from the arterioles within the

mTT. In hamster retractor muscle, about two-thirds of the net decline in SaO₂ occurs in the arterioles under resting conditions ([Swain and Pittman, 1989](#)). Similar studies, however, have not been reported in the brain, although the amount of oxygen unloaded during the NIRS measurement is thought to be <6% ([Elwell et al., 1994](#)).

Another assumption of the NIRS method is that the CBF does not change with the induction of mild hypoxia (SaO₂ > 85%) required to make these measurements. There is no overall change in CBF during small changes in PaO₂ in humans ([Siesjo, 1978](#)). Likewise [Kogure et al. \(1970\)](#) found that CBF did not increase until the PaO₂ was below 60 mm Hg in dogs, although [Traystman et al. \(1978\)](#) found a linear relationship between a stepwise reduction in O₂ content and CBF. We found that CBF did not change overall during most hypoxic runs, although fluctuations in CBF_v occurred during most measurements. In most cases there was an initial increase in CBF_v as the animal was made hypoxic, followed by a reduction of CBF_v with the administration of 100% O₂ ([Fig. 1](#)). There was up to a median of 12% change in CBF_v during the hypoxic runs, although the percentage change did not correlate with the change in O₂ content, possibly because differences in the depth of anesthesia between the animals.

We are unable to calculate the overall limits of agreement ([Bland and Altman, 1986](#)) between the CBF_{NIRS} and the other measures of CBF, since each animal had a different number of acceptable NIRS measurements. The CBF_w provided measurements of regional CBF but has an intrinsic variability (median 11.6%) that makes comparisons difficult. The CBF_v allowed us to identify the changes in the CBF during the CBF_{NIRS} measurements and compare single CBF_{NIRS} measurements. The CBF_v, however, measures global CBF, while the CBF_{NIRS} is thought to be a measure of regional blood flow.

In conclusion, NIRS detects blood flow in the brain in most subjects, but measurement of CBF_{NIRS} in the reflectance mode, using oxygen as an intravascular tracer is inaccurate, particularly at high CBF values ([Fig. 3](#)). Furthermore, many of the measurements have to be discarded and there is a high CV of the remaining measurements. The causes of the inaccuracy are likely to be a combination of factors. We have identified the variable contribution of the extracranial compartment and changes in CBF induced by the NIRS measurements to be responsible for some of the inaccuracy and the quality of the saturation signal to be important in determining the number of acceptable measurements. However, diffusion of oxygen within the mTT and changes in the DPF during the measurements may also contribute. The major differences between this validation study and others that showed a better correlation ([Skov et al., 1991](#); [Bucher et al., 1993](#)) were higher flow values, shorter mTT, and greater contamination because of a reflection geometry and thicker, denser extracranial tissues. To improve the accuracy and reduce the variability of the CBF_{NIRS} measurements in older subjects with higher flows, the DPF should be measured at the time of the CBF measurement, instruments with faster sampling times and lower noise need to be developed, and a greater increase in intravascular marker needs to be produced in a shorter time period.

[Top of page](#)

References

References

1. Bland JM & Altman DG. (1986) Statistical methods for assessing agreement between two methods of clinical measurement. *Lancet* **1**: 307–310.
2. Bucher HU, Edwards AD, Lipp AE & Duc G. (1993) Comparison between near infrared spectroscopy and ¹³³Xenon clearance for estimation of cerebral blood flow in critically ill preterm infants. *Pediatr Res* **33**: 56–60.
3. Cope MC. 1991 The development of a near infrared spectroscopy system and its application for non-invasive monitoring of cerebral blood and tissue oxygenation in the newborn infant. (Ph.D. thesis, University of London).
4. Delpy DT, Arridge SR, Cope M, Edwards D, Reynolds EO, Richardson CE, Wray S, Wyatt J & van der Zee P. (1989) Quantitation of pathlength in optical spectroscopy. *Adv Exp Med Biol* **248**: 41–46.
5. Edwards AD, Wyatt JS, Richardson C, Delpy DT, Cope M & Reynolds EO. (1988) Cotside measurement of cerebral blood flow in ill newborn infants by near infrared spectroscopy. *Lancet* **2**: 770–771.
6. Elwell CE, Cope M, Edwards AD, Wyatt JS, Delpy DT & Reynolds EO. (1994) Quantification of adult cerebral hemodynamics by near-infrared spectroscopy. *J Appl Physiol* **77**: 2753–2760.
7. Essenpreis M, Cope M, Elwell CE, Arridge SR, van der Zee P & Delpy DT. (1993) Wavelength dependence of the differential pathlength factor and the log slope in time-resolved tissue spectroscopy. *Adv Exp Med Biol* **333**: 9–20.
8. Fallon P, Roberts I, Kirkham FJ, Elliott MJ, Lloyd-Thomas A, Maynard R & Edwards AD. (1993) Cerebral hemodynamics during cardiopulmonary bypass in children using near-infrared spectroscopy. *Ann Thorac Surg* **56**: 1473–1477.
9. Ferrari M, Hanley DF, Wilson DA & Traystman RJ. (1990) Cerebral cytochrome C-oxidase copper band quantification in perfluorocarbon exchange transfused cats. *Adv Exp Med Biol* **277**: 85–93.
10. Ferrari M, Wilson DA, Hanley DF & Traystman RJ. (1992) Effects of graded hypotension on cerebral blood flow, blood volume, and mean transit time in dogs. *Am J Physiol* **262**: H1908–H1914.
11. Ferrari M, De Blasi RA, Safoue F, Wei Q & Zaccanti G. (1993) Towards human brain near infrared imaging: time resolved and unresolved spectroscopy during hypoxic hypoxia. *Adv Exp Med Biol* **333**: 21–31.
12. Heymann MA, Payne BD, Hoffman JI & Rudolph AM. (1977) Blood flow measurements with radionuclide-labelled particles. *Prog Cardiovasc Dis* **20**: 55–79.
13. Hiraoka M, Firbank M, Essenpreis M, Cope M, Arridge SR, van der Zee P & Delpy DT. (1993) A Monte Carlo investigation of optical pathlength in homogeneous tissue and its application to near-infrared spectroscopy. *Phys Med Biol* **38**: 1859–1876.
14. Jobsis FF. (1977) Noninvasive, infrared monitoring of cerebral and myocardial oxygen sufficiency and circulatory parameters. *Science* **198**: 1264–1267.
15. Kogure K, Scheinberg P, Reinmuth OM, Fujishima M & Busto R. (1970) Mechanisms of cerebral vasodilatation in hypoxia. *J Appl Physiol* **29**: 223–229.
16. Marcus LL, Heistad DD, Ehrhardt JC & Abboud FM. (1976) Total and regional cerebral blood flow measurement with 7-, 10-, 15-, 25-, 50- μ m microspheres. *J Appl Physiol* **40**: 501–507.
17. Matcher SJ, Elwell CE, Cooper CE, Cope M & Delpy DT. (1995) Performance comparison of several published tissue near-infrared spectroscopy algorithms. *Anal Biochem* **227**: 54–68.
18. Rapela CE & Green HD. (1964) Autoregulation of canine cerebral blood flow. *Circ Res* **15**:

- 205–211.
19. Seisjo BK. 1978 *Brain Energy Metabolism* Chichester: Wiley (pp) 422–426.
 20. Skov L, Pryds O & Greisen G. (1991) Estimating cerebral blood flow in newborn infants: comparison of near infrared spectroscopy and ¹³³Xe clearance. *Pediatr Res* **30**: 570–3.
 21. Swain DP & Pittman RN. (1989) Oxygen transport in the microcirculation of hamster retractor muscle. *Am J Physiol* **256**: H247–H255.
 22. Traystman RJ & Rapela CE. (1975) Effect of sympathetic nerve stimulation on cerebral and cephalic blood flow in dogs. *Circ Res* **36**: 620–630.
 23. Traystman RJ, Fitzgerald RS & Loscutoff SC. (1978) Cerebral circulatory responses to arterial hypoxia in normal and chemodenervated dogs. *Circ Res* **42**: 649–657.
 24. van der Zee P, Cope M, Arridge SR, Essenpreis M, Potter LA, Edwards AD, Wyatt JS, McCormick DC, Roth SC, Reynolds EO & Delpy D. (1992) Experimentally measured optical pathlengths for the adult head, calf and forearm and the head of the newborn infant as a function of inter optode spacing. *Adv Exp Med Biol* **316**: 143–153.

[Top of page](#)

Acknowledgements

We thank Professor R. Royall for statistical advice.